

STICHTING VOOR BODEMKARTERING
WAGENINGEN

REPORT ON BASIC EXERCISES ON MICROPEDOLOGY
IN THE SECTION OF MICROPEDOLOGY OF THE DUTCH
SOIL SURVEY INSTITUTE IN WAGENINGEN

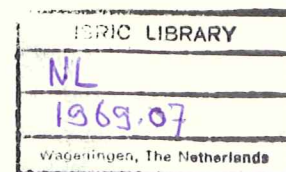


By Shizuo NAGATSUKA

ISRIC LIBRARY

NL 1969.07

Optic-Volumetric Measurement of Soil Components



1. Point-count method

1.1 Method

Three different soil components, sand grain, organic matter and air, in a mammoth-sized thin section (Jongerius and Heintzberger, 1963) were measured under a polarizing microscope with a Zeiss Integration Eyepiece I (X 8 magnification). 25 points are marked out in a grid in the eyepiece to form equilateral triangles (Fig. 1). The different components distinguished are identified optically below each point in the grid. These counts are repeated for 154 "sites" (14 horizontally, 11 vertically, these numbers are sufficient for the low magnification used; at high magnification the number of counts must be much higher) distributed to form the corners of equal squares (5 by 5 mm) on the thin section (Fig. 2).

From the total point scores for the different components, their volume percentages were directly calculated. Namely, percentage by number was used directly as percentage by volume (Table 1). The mean absolute errors of the figures were obtained from a nomogram (Carl Zeiss).

The distance between two grid points in the eyepiece was 650μ in case of 8 X 4 magnification. Using this distance as a measure scale, the diameter of pores under a grid point was estimated and classified into 5 classes, that is, less than $1/4$, $1/4 - 1/3$, $1/3 - 1/2$, $1/2 - 1$, more than 1 parts of the distance between two grid points respectively. In this way, the volumes of different diameter classes of pores were determined.

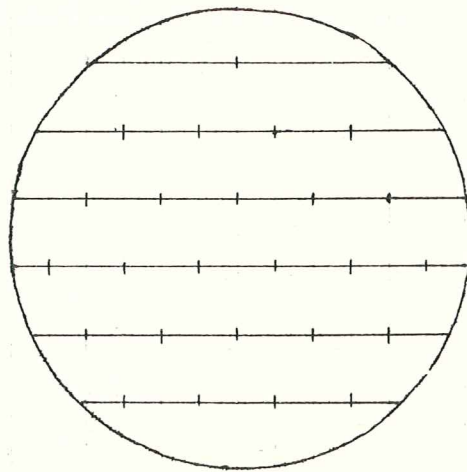


Fig. 1 A grid in a Zeiss integration eyepiece I.

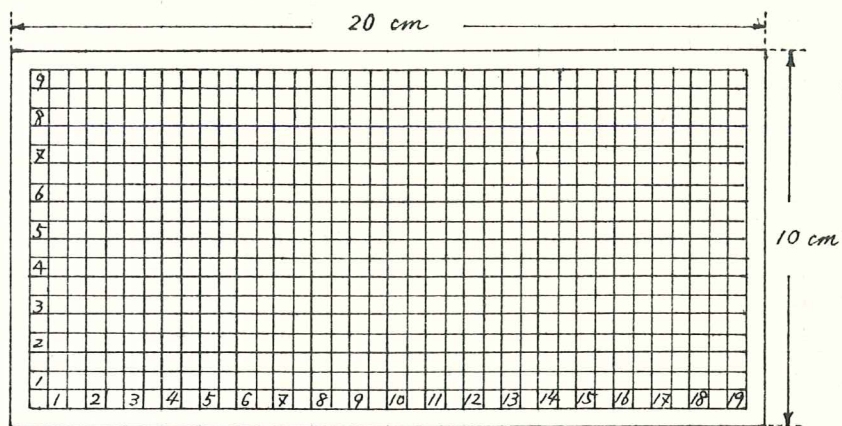


Fig. 2 The corners of equal squares (5 by 5 mm)

Table 1. Point scores of different components

Depth (cm)	site Components	1	2	3	4	5	6	7	8	9	10	11	12	13	14	Total	%
17	sand	7	10	13	11	14	11	13	14	14	15	13	18	18	13	184	52.6 \pm 1.8
	O. M.	5	3	2	4	0	7	8	1	4	3	6	4	2	3	52	14.8 \pm 1.3
	air	13	12	10	10	11	7	4	10	7	7	6	3	5	9	114	32.6 \pm 1.7
18	sand	15	14	18	10	12	6	13	16	12	11	15	14	13	8	177	50.6 \pm 1.8
	O. M.	2	2	5	10	5	10	4	4	7	3	3	6	8	3	72	20.6 \pm 1.4
	air	8	9	2	5	8	9	8	5	6	11	7	5	4	14	101	28.8 \pm 1.6
19	sand	14	13	10	16	14	14	12	11	16	14	15	18	14	14	195	55.6 \pm 1.8
	O. M.	4	6	6	7	2	5	4	6	6	5	5	3	3	2	64	18.4 \pm 1.4
	air	7	6	9	2	9	6	9	8	3	6	5	4	8	9	91	26.0 \pm 1.6
20	sand	14	18	13	16	8	12	11	10	11	13	14	15	12	13	180	51.2 \pm 1.8
	O. M.	6	2	4	4	7	10	8	7	6	6	4	5	7	6	82	23.6 \pm 1.5
	air	5	5	8	5	10	3	6	8	8	6	7	5	6	6	88	25.2 \pm 1.6
21	sand	12	8	16	10	14	12	12	12	12	11	15	14	18	10	176	50.4 \pm 1.8
	O. M.	6	3	6	8	5	6	3	7	8	10	4	7	1	3	77	22.0 \pm 1.5
	air	7	14	3	7	6	7	10	6	5	4	6	4	6	12	97	27.6 \pm 1.6
22	sand	9	12	14	12	11	11	6	3	11	17	11	8	17	11	153	43.7 \pm 1.8
	O. M.	4	6	8	6	4	4	8	6	8	5	3	6	4	7	79	22.6 \pm 1.5
	air	12	7	3	7	10	10	11	16	6	3	11	11	4	7	118	33.7 \pm 1.7
23	sand	12	13	8	12	11	15	13	10	13	10	17	15	10	16	175	50.0 \pm 1.8
	O. M.	5	3	6	7	4	3	7	8	6	5	7	6	8	4	79	22.6 \pm 1.5
	air	8	9	11	6	10	7	5	7	6	10	1	4	7	5	96	27.4 \pm 1.6
24	sand	8	8	9	14	14	12	13	10	12	11	8	17	14	15	165	47.2 \pm 1.8
	O. M.	6	4	6	5	5	5	7	6	2	10	6	4	3	6	75	21.4 \pm 1.5
	air	11	13	10	6	6	8	5	9	11	4	11	4	8	4	110	31.4 \pm 1.6
25	sand	11	14	15	13	11	13	17	17	15	11	12	10	11	18	188	53.7 \pm 1.8
	O. M.	3	3	5	4	4	4	3	4	4	8	2	7	7	4	62	17.7 \pm 1.4
	air	11	8	5	8	10	8	5	4	6	6	11	8	7	3	100	28.6 \pm 1.6
26	sand	9	11	9	14	6	12	14	14	12	10	18	13	12	12	166	47.4 \pm 1.8
	O. M.	6	5	3	4	8	8	5	8	6	7	1	7	4	8	80	22.9 \pm 1.5
	air	10	9	13	7	11	5	6	3	7	8	6	5	9	5	104	29.7 \pm 1.6
27	sand	7	9	13	15	12	15	12	17	8	19	13	11	8	15	174	49.7 \pm 1.8
	O. M.	6	6	8	4	6	3	4	3	3	3	4	6	6	3	65	28.5 \pm 1.4
	air	12	10	4	6	7	7	9	5	14	3	8	8	11	7	111	31.8 \pm 1.7

1.2 The sample examined

The soil sample comes from A_p horizon of an asparagus field at Meldersloo, in the Netherlands (Sample No. A1 50484). The position where the sample was taken from is shown in Fig.3. The upper 6 cm of the sample belongs to ridge part and the lower 9 cm to the root zone.

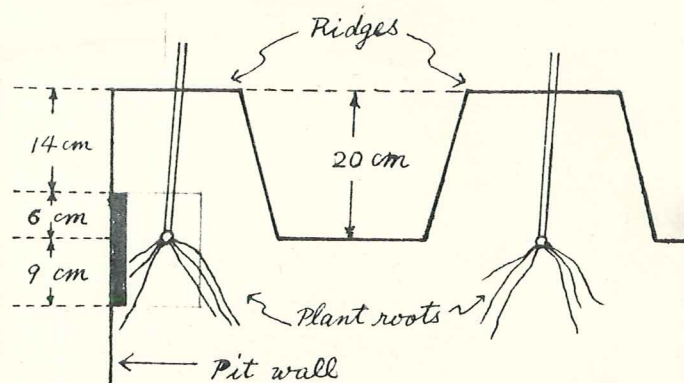


Fig.3 The position of the sample

1.3 Results of the measurement

Fig.4 and Fig.5 show the volume distribution of sand, organic matter and air.

The volume of air in the ridge part gradually decreases from the surface showing the minimum value at the plant depth, and again gradually increases in the root zone, showing the maximum value at 2cm below the plant depth. On the other hand, the volume of sand shows the maximum value at the depth of 19 cm in the ridge part and the minimum value at the depth of 2cm below the plant depth where the volume of air is maximum. The volume of organic matter gradually increases with depth in the ridge part, while in the root zone it is rather homogeneous until 24 cm depth.

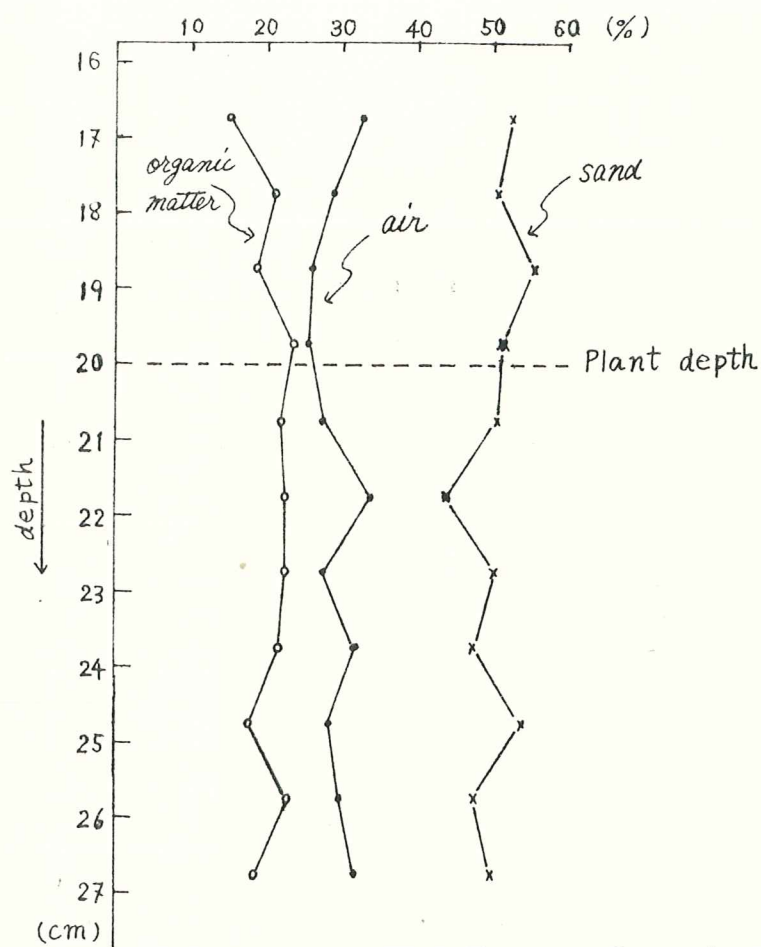


Fig. 4 Volume distribution of sand, organic matter and air.

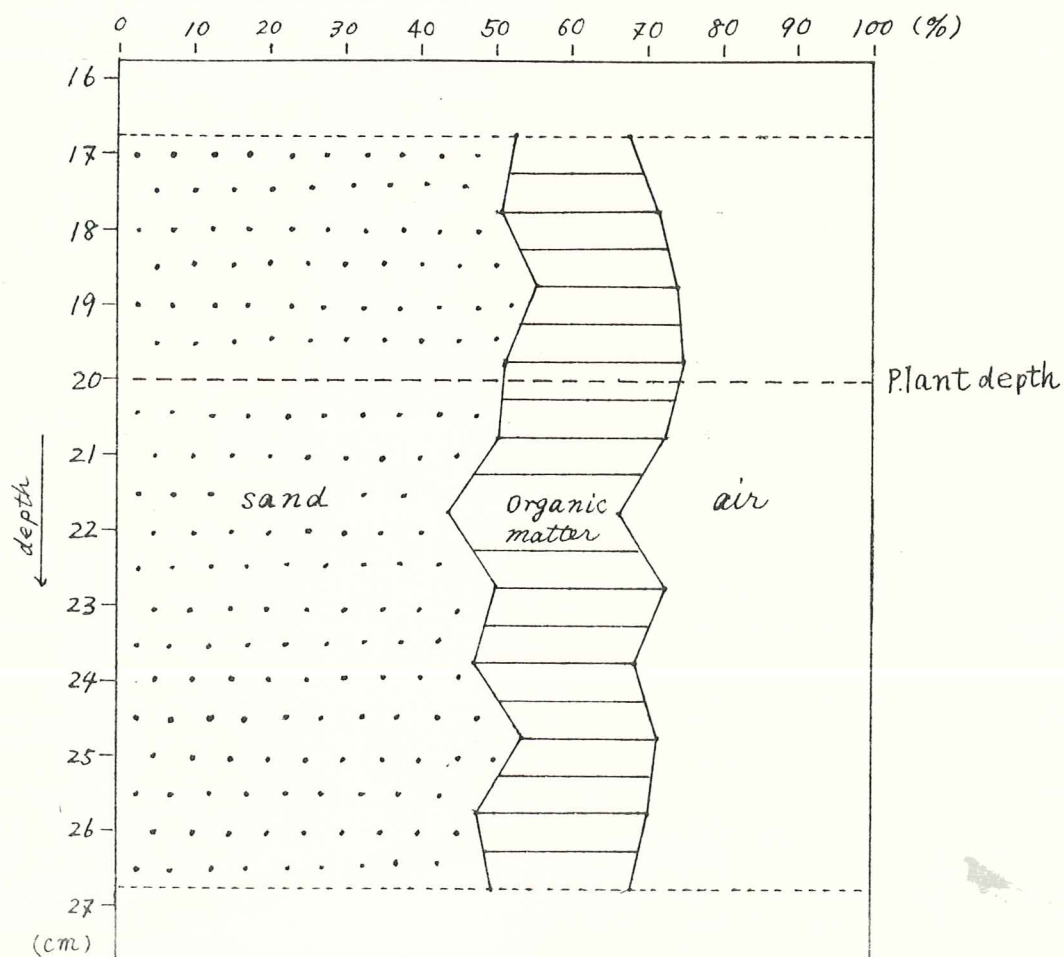


Fig. 5. Volume distribution of sand, organic matter and air.

To know the change of pore size distribution by ploughing, ~~and mixing of soil material by it~~, the pore size distribution at the depth of 20 cm (in the ridge part) and 22 cm (in the root zone) were compared. The results are shown in Fig.6 and Fig.7.

Comparing the total porosity and the pore size distribution at the depth of 20 cm with those at the depth of 22 cm, the total porosity of the former decreases from 34.0% of the latter to 23.4%, whereas percentage of pore size between 217-650 μ decreases and percentage of pore size less than 217 μ increases.

1.4 Conclusion

By the optic-volumetric measurement of a mammoth-sized thin section from A_p horizon of an asparagus field, it was shown that the total porosity at the plant depth in the ridge part is less than that of the part under the plant depth. At the same time, at the plant depth, percentage of pore size between 217 and 650 μ decreases and percentage of pore size less than 217 μ increases as compared with those in the part under the plant depth. This change of total porosity and the pore size distribution may be considered to be caused by pressing when the plant depth is ploughed.
_{to}

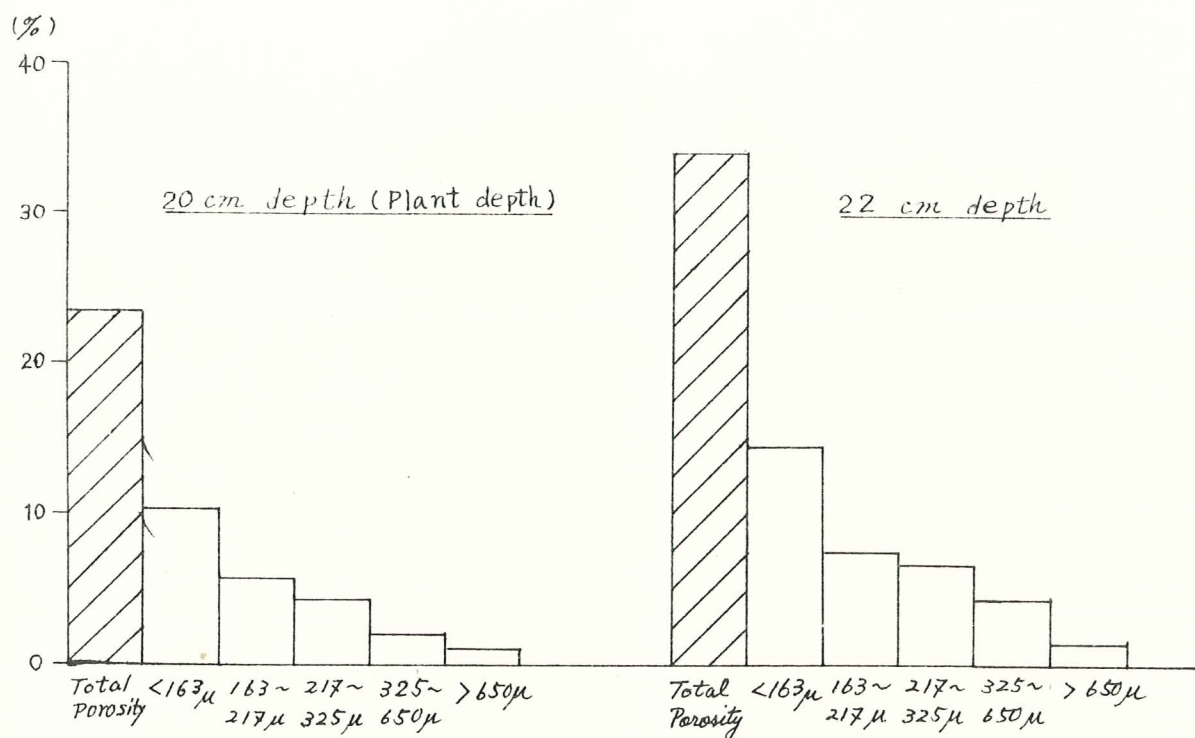


Fig. 6 Pore size distribution (Total mass basis)

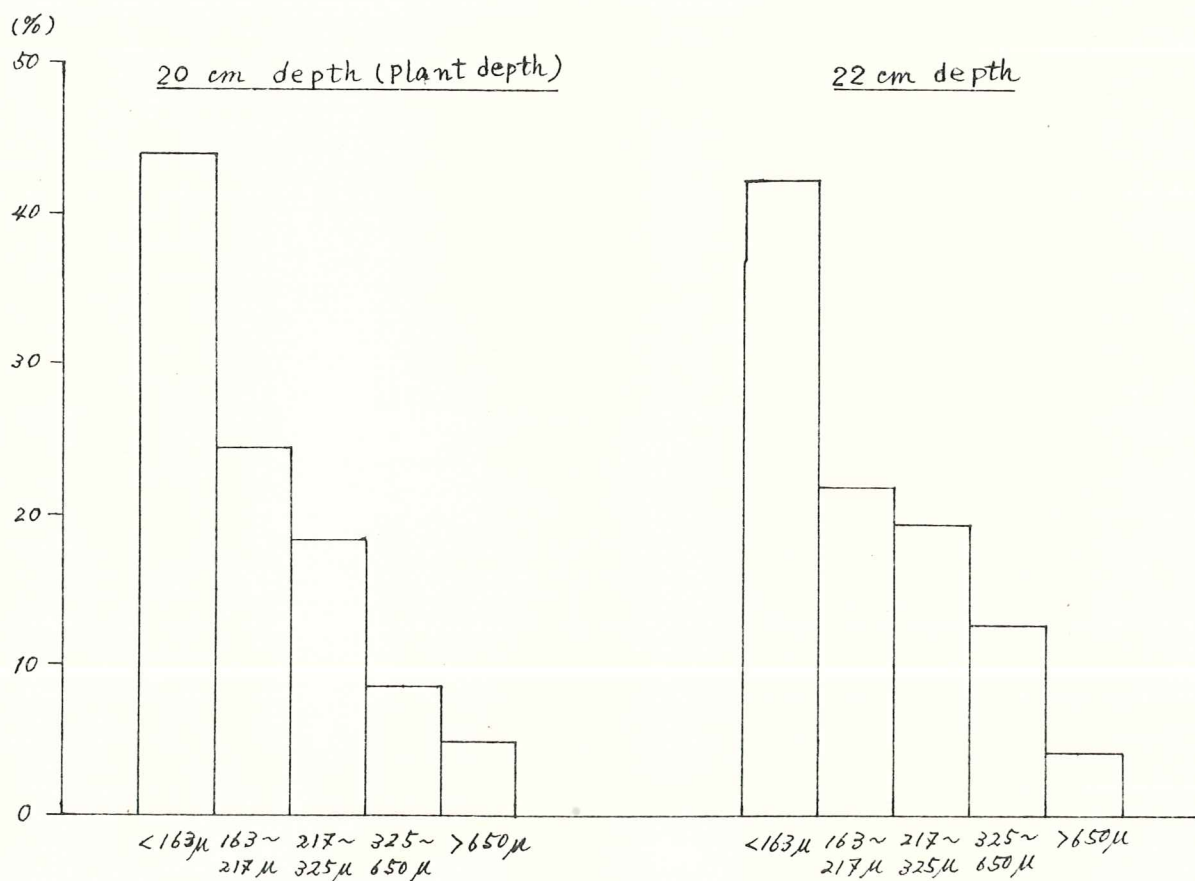


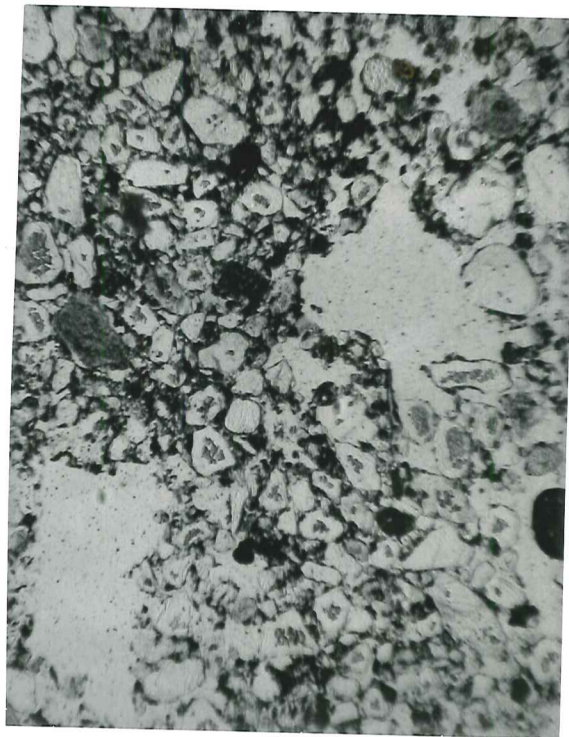
Fig. 7 Pore size distribution (Total porosity basis)



500 μ

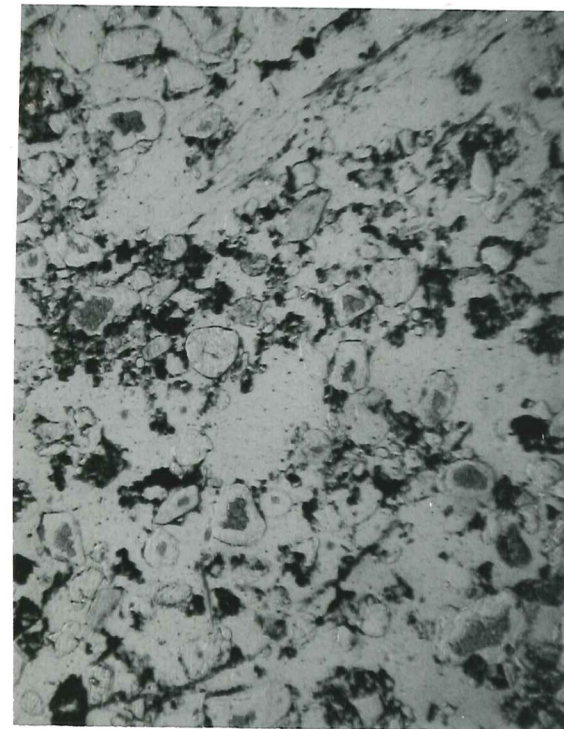
Photo 1. 17 cm depth. X 40

black part = organic matter



500 μ

Photo 2. 20 cm depth (plant depth) X 40



500 μ

photo 3. 22 cm depth. X 40

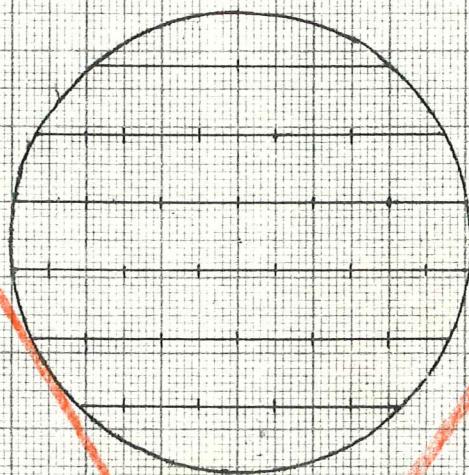


Fig. 1 A grid in a Zeiss integration eyepiece I.

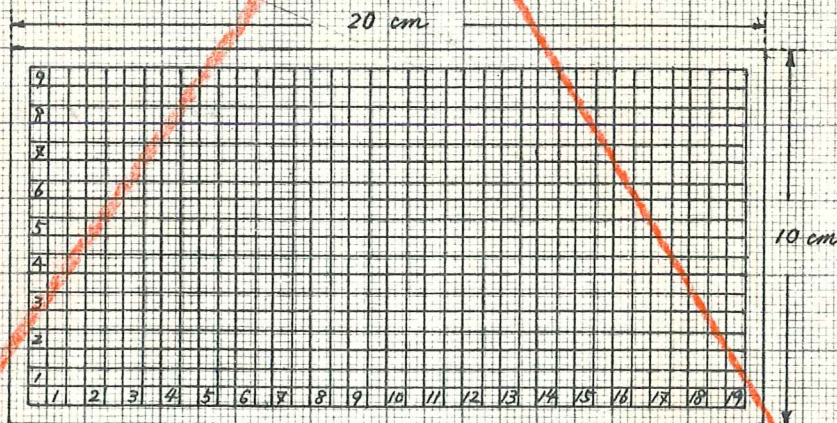


Fig. 2 The corners of equal squares (5 by 5 mm)

2. Line-count method

2.1 Method

Measurement of the pore size distribution of a soil thin section of another asparagus-soil was done using a Zeiss particle size analyser(TGZ3).

A differentiated structure photograph(9 by 12cm, X 50) was taken of a mammoth-sized thin section according to the photographic technique developed by Jongerius (Jongerius, 1963~~4~~). On this photograph, sand grains show up black, the fine mineral fractions and organic matter white and the pores grey.

The photo is fixed with scotch tape to a transparent sheet marked with points to form an extended grid. The spacing⁺ between the points was 2.5mm, giving 1566 points to a photograph of 9 by 12cm.

+ : The spacing most commonly used is half a cm, giving 446 points to a photo of 9 by 12cm.

The photo is systematically traversed along the (imaginary) horizontal lines connecting the grid points. Where a pore covers one or more gridpoints, the diaphragm is adjusted so that the section of the line across the pore forms the diameter of the light-circle.

For every gridpoint on the line section the foot-pedal is then pushed once.(Jongerius, 1963~~4~~).

In this way, the numbers of grid points covered by pores are scored mechanically. At the same time the diaphragm diameter is recoded fractionately for 48 diameter classes.

2.2 Culculation

The data of measurement are shown in Table 2. From these data, the total porosity and the pore size distribution were culculated in the following way;

Table 2. A score record by a Zeiss particle size analyser

diameter class site		< 100 μ								100 ~ 200 μ								200 ~ 300 μ								300 ~ 500 μ										> 500 μ													
		1	2	3	4	5	6	7	8	9	10	11	12	13	14	15	16	17	18	19	20	21	22	23	24	25	26	27	28	29	30	31	32	33	34	35	36	37	38	39	40	41	42	43	44	45	46	47	48
A		2	2	3	3	4																																											
B			1	1	2	2																																											
C		1		6		1	2						4																																				
D			1		1	2	2	2		3																																							
E		1		3					5		6																																						
F		3	1	2	2				3		3										3																												
G		1	2			2	2	2	3		3										3																												
H		1		1	1				2																																								
J		1	1										3																																				
K		1				2	1			3																																							
L		1	3	2	3	1	3	2																																									
M				2	3				2	2	3							4																															
N		2	2	1			2	2	3										5																														
O			2					2				4	4											6																									
P			3	1		6																																											
Q		2	6	1		3																																											
R		1	2	3	2					2																																							
S		2		4	3	2	2	5																																									
T		1	1		3																																												
U		1	2	1		2	2	2		3																																							
V		2		1		2			2	6	1	1		3	1	5	2																																
W		1	1	2		4		3	4	3	3																																						
X			2	1	2				3				3																																				
Y					1		2	3	3			3																																					
Z		1		3	4	3				3																																							
AA			4	1								4		3																																			
BB			2			2			3	3		1	4																																				
CC				1		4	4	2			3			2	3																																		
DD					2	2	4			5																																							
EE				1	2	1	2				2																																						
FF		1	1	1					2	6		4																																					
GG				2	3					2																																							
HH		1	1	2				1																																									
JJ		1			3	3																																											
KK		1	1	2		3	2	2	5																																								
LL					1	1		2			3			7				5																															
li		28	41	48	41	52	31	27	42	38	30	26	14	22	13	12	2	18	10	0	12	10	5	7	0	6	4	6	9	0	0	0	8	0	9	0	9	0	0	0	10	0	0	7	0	0	1		
Σli		Σ _{i=1} ⁸ li = 310								Σ _{i=9} ¹⁶ li = 157								Σ _{i=17} ²⁵ li = 68								Σ _{i=26} ⁴³ li = 62										Σ _{i=44} ⁴⁸ li = 1													

$$P = \frac{n}{N} \times 100 = \frac{598}{1566} \times 100 = 38.2 \%$$

where;

P : Total porosity

N : Total number of grid points,

n : The number of grid points covered by pores,

$$\text{Percentage less than } 100\mu = P \times \frac{\sum_{i=1}^{16} l_i}{n} = 38.2 \times \frac{310}{598} = 19.8 \%$$

$$\text{Percentage } 100-200\mu = P \times \frac{\sum_{i=17}^{25} l_i}{n} = 38.2 \times \frac{157}{598} = 10.0 \%$$

$$\text{Percentage } 200-300\mu = P \times \frac{\sum_{i=26}^{43} l_i}{n} = 38.2 \times \frac{68}{598} = 4.3 \%$$

$$\text{Percentage } 300-500\mu = P \times \frac{\sum_{i=44}^{48} l_i}{n} = 38.2 \times \frac{62}{598} = 4.0 \%$$

$$\text{Percentage more than } 500\mu = P \times \frac{\sum_{i=49}^{48} l_i}{n} = 38.2 \times \frac{1}{598} = 0.1 \%$$

Where;

l_i = Frequency of each diameter class,

i : Diameter class,

2.3 Result

The pore size distribution of the sample is shown in

Fig. 8.



Fig 8. The pore size distribution

3. Measurement of particle size distribution by the Quantimet

3.1. Introduction

The invention of the Quantimet Image Analysing Computer (Q.T.M.) has enormously increased the speed of particle analysis in the field of metallurgy, ceramics, mineralogy, biology, soil science and many other research works.

The instrument makes it possible to measure automatically three parameters of the features in a field of view, namely, area, projection and number. These data are directly displayed on the meter and the images are shown during measurement simultaneously on the television monitor. From this detailed information, a very wide range of secondary measurements can be derived such as form factors, mean sizes, form factor distributions, mean linear intercept, re-entrance factors, perimeter and interface length, fibre diameters and length etc.

For more detailed information about the principle of measurement, arrangement and electric circuit of the instrument, reference will be made to specialized papers (Cole, 1966, Fisher, 1966).

The application of the Q.T.M. to the study of micropedology has made possible the quantitative insight into microstructural features of soil. Jongerius et al have developed a classification system of soil micro-structures based on detailed quantitative analysis of pore characteristics using the Q.T.M. (by personal communication).

The outline of the measuring method of soil pores by the Q.T.M. will be mentioned in the following pages.

3.2 Specimen preparation

A mammoth-sized thin section for the measurement of pore size is prepared in case of sandy material somewhat different way from that used in case of fabric analysis, because the transmitted light passes through the sand grains in the same way as through the uncoloured plastic.

The impregnant (Vestopal H) used contains 3% transparent green dye (PC44-954W) from Ferro N.V. (Rotterdam). This dye can be dissolved in Vestopal H homogeneously and does not show any aggregate of dye which interfere light transmission through pores.

It is not necessary for the thin section to be polished so thin in this case, usually 40 μ of thickness is enough for the purpose.

It is not necessary to cover the sample with cover glass, neither.

3.3 Outline of the procedure of pore measurement

As the more exact procedure is mentioned in the instruction manual (Metals Research LTD.), only the outline of procedure will be mentioned here.

- 1) Switch on the Mains, the Q.T.M. and the light source(Lamp 1 and 2, dark field incident light) switches. Set the lamp rheostat in the position 8 and allow about one minute for the monitor tube to warm up. Switch the Display switch to Image. Wait several ten minutes till the whole electric circuit get to stable state.
- 2) Set the Function switch to Area, the Detection Polarity to Black, the Resolution to Min. and the Threshold to zero. Switch the Display switch to Superimposed Direct or Banded. Place a glass plate with square grids on the specimen support plate on the top of the epidiascope. Adjust the Blank Frame set-up controls on the left-hand preset panel to give the desired blank frame size (in this case 10 X 15 mm) and position.

- 3) Take off the glass plate, then switch on the Display switch to Meter, turn the meter range switch to maximum sensitivity(0.33) and set the meter zero correctly. Set the range switch to the highest range (100 % F.S.D.), advance the Threshold conyrol to saturate. If a very small blank frame has been selected, it may not be possible to get full scale deflection in the area or projection mode at 100 % or one line respectively, in which case set for 1/2 scale or some other convenient fraction and modify the readings appropriately.
- 4) Switch the Display switch to Superimposed Direct, then place the mammoth-sized thin section on the specimen support plate, turn the detection control till the features are superimposed, then switch the Display switch again to Meter and read the meter (Total area expressed as percentage read of the blank frame; a).
- 5) Switch the Function switch to Dense Projection, then read the meter (Total projection; P_t).
 Rotate the Minimum Chord control and read the meter at every 0.20 scale at this magnification ($\pm 20 \times$). Every 0.20 scale correspond in this case to 100 μ . As the Minimum Chord control is advanced, the shorter chord length will disappear. (range 90 - 5000 μ)

3.4 Calculation

The total actual area(1) and the area of each pore size class(2) are calculated as follows;

$$A_t = \frac{A \times L \times H}{M^2} \quad (1)$$

where;

A_t : Actual area covered.

H : Blank frame height on the monitor.

L : Blank frame width on the monotor.
A : Percentage read on meter expressed as a fraction.
M : Magnification.

$$a = (P_{0,1} \text{ etc.} - P_{1,2} \text{ etc.}) \times d \quad (2)$$

where;

a : Area of each diameter class expressed as $\mu^2 \times 10^4$

$P_{0,1}$ etc : Projection value read on meter at every
0.20 scale setting.

d : Average of each diameter class.

If the specimen is three dimensional and is uniform in its composition throughout its depth, then the percentage area as read from the Quantimet is identical to the volume fraction.

An example of the measurement of pore size distribution of a mammoth-sized thin section is shown in Table 3 and Fig. 9.

Table 3. A measurement of pore size distribution by the Q. T. M.

Minimum chord setting	Diameter class (μ)	Read * P-value	Difference $P_i - P_{i+1}$ (A)	Mean diameter (μ) (B)	A x B (x $10^4 \mu^2$)	Area of pore size class	Volume %
0.00		2.18 (P ₀)					
0.20	< 100 μ	2.10	0.08	50	4.00	4.00	0.2
0.40	100 - 200	1.56	0.54	150	81.00	81.00	3.4
0.60	200 - 300	1.13	0.43	250	107.50	107.50	4.5
0.80	300 - 400	0.84	0.29	350	107.50	182.50	7.7
1.00	400 - 500	0.66	0.18	450	81.00		
1.20	500 - 600	0.59	0.07	550	38.50		
1.40	600 - 700	0.55	0.04	650	26.00		
1.60	700 - 800	0.54	0.01	750	7.50	90.00	3.8
1.80	800 - 900	0.53	0.01	850	8.50		
2.00	900 - 1000	0.52	0.01	950	9.50		
2.20	1000 - 1100	0.51	0.01	1050	10.50		
2.40	1100 - 1200	0.49	0.02	1150	23.00		
2.60	1200 - 1300	0.49	0.00	1250	—		
2.80	1300 - 1400	0.49	0.00	1350	—		
3.00	1400 - 1500	0.49	0.00	1450	—	87.00	3.6
3.20	1500 - 1600	0.48	0.01	1550	15.50		
3.40	1600 - 1700	0.48	0.00	1650	—		
3.60	1700 - 1800	0.48	0.00	1750	—		
3.80	1800 - 1900	0.47	0.01	1850	18.50		
4.00	1900 - 2000	0.46	0.01	1950	19.50		
4.20	2000 - 2100	0.46	0.00	2050	—		
4.40	2100 - 2200	0.46	0.00	2150	—		
4.60	2200 - 2300	0.46	0.00	2250	—		
4.80	2300 - 2400	0.45	0.01	2350	23.50		
5.00	2400 - 2500	0.44	0.01	2450	24.50	132.50	5.6
5.20	2500 - 2600	0.44	0.00	2550	—		
5.40	2600 - 2700	0.43	0.01	2650	26.50		
5.60	2700 - 2800	0.43	0.00	2750	—		
5.80	2800 - 2900	0.42	0.01	2850	28.50		
6.00	2900 - 3000	0.41	0.01	2950	29.50		
6.20	3000 - 3100	0.40	0.01	3050	30.50		
6.40	3100 - 3200	0.40	0.00	3150	—		
6.60	3200 - 3300	0.40	0.00	3250	—		
6.80	3300 - 3400	0.39	0.01	3350	33.50		
7.00	3400 - 3500	0.38	0.01	3450	34.50		
7.20	3500 - 3600	0.37	0.01	3550	35.50		
7.40	3600 - 3700	0.36	0.01	3650	36.50		
7.60	3700 - 3800	0.35	0.01	3750	37.50		
7.80	3800 - 3900	0.31	0.04	3850	154.00	1689.50	71.2
8.00	3900 - 4000	0.31	0.00	3950	—		
8.20	4000 - 4100	0.26	0.05	4050	202.50		
8.40	4100 - 4200	0.16	0.10	4150	415.00		
8.60	4200 - 4300	0.13	0.03	4250	127.50		
8.80	4300 - 4400	0.10	0.03	4350	130.50		
9.00	4400 - 4500	0.06	0.04	4450	178.00		
9.20	4500 - 4600	0.01	0.05	4550	227.50		
9.40	4600 - 4700	0.00	0.01	4650	46.50		

2.18
(= P_t)

2374.00
(23.74 mm²) **

100.0 %

* These figures were obtained by multiplying the actual meter readings by 2, because the meter scale was set for $\frac{1}{2}$ of full scale.

** Total pore area = $\frac{10 \text{ mm} \times 15 \text{ mm} \times 16.5}{100} = 24.75 \text{ mm}^2$
Actual.

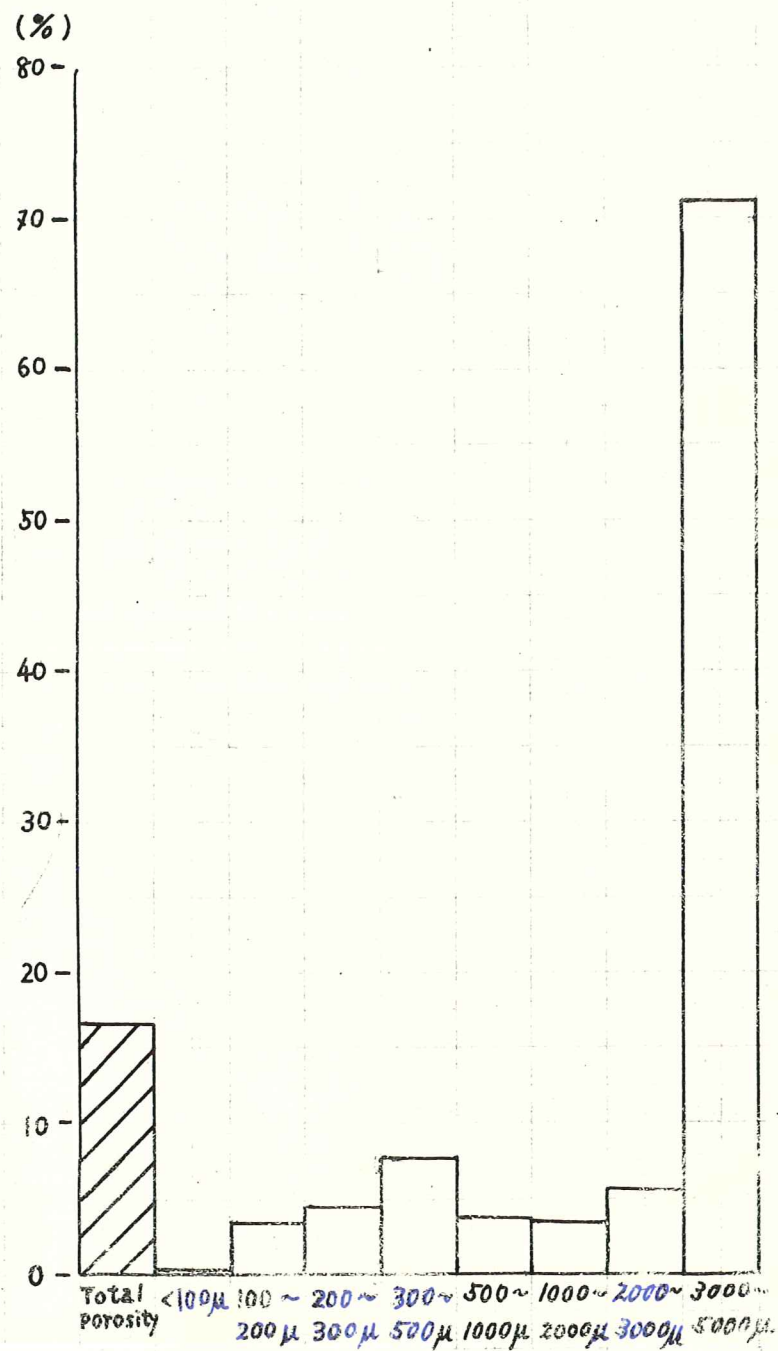


Fig. 9 Pore size distribution measured by the Q.T.M.

Micromorphological observation of Chernozem, Dark meadow soil
and Black soil of Humic Gley origin of Yugoslavia

1. Introduction

The purpose of this investigation is to obtain informations about the micromorphological characteristics of soils with deep black A-horizon, namely, Chernozem, Dark meadow soils and Black soils of Humic Gley origin, in Yugoslavia.

2. Method.

Clods which have well-preserved natural macrostructures were used as samples to prepare thin-sections for micromorphological observation under a petrographic microscope.

The thin sections were prepared, using Vestopal H as a impregnant, according to the method described by Jongerius and Heintzberger(1963). The terms used in the description of micromorphological features except those for humus forms, are based on those which have been established by Brewer (1964).

3. The samples

The samples come from Novi Sad, Yugoslavia.

Some characteristics of the samples are shown in table 1.

Table 1. The samples examined

Sample No.	Kind of soils	Depth
1.	Chernozem (top soil)	5 - 15 cm
2.	Chernozem (sub soil)	35 - 45 cm
3.	Dark meadow soil	0 - 40 cm
4.	Black soil of Humic Gley origin (Sandy)	20 - 40 cm
5.	Black soil of Humic Gley origin (Heavy mineral soil)	20 - 40 cm

One of the plant tissues shows a characteristic cell structure of monocotyledon, the rim of which is disintegrated and is surrounded with phytoliths and fecal pellets (excretions).

This humusform may be considered as a transition type between mull and anmoor. It may not be considered as a transition type between moder and mull, because of the strong bindings between organic and mineral material.

C) Black soils of Humic Gley origin (Photo4 and 5)

The thin sections of sample No.4 and 5 show dark brown to black finely divided humus substances with greyish shade, which are well mixed with clay to form clay-humus complex. Besides clay-humus complex, many dark domains(approximately 50 μ in diameter) occur, consisting predominantly of poorly humified organic matter.

And furthermore light coloured plant tissues are present in the voids or on the surfaces of peds.

The two thin sections display different distribution patterns of the dark domains. In sandy soil(No.4), the domains are distributed rather homogeneously, but in clayey soil(No.5), the domains are locally concentrated among the dark brown finely divided clay-humus complex to form big dark clusters. This heterogeneous distribution pattern may suggest the relatively heterogeneous physico-chemical environmental conditions such as redox potential in the clayey soil.

From the above microscopic observations, the humusforms of the two samples were identified as "anmooric", and to distinguish the different distribution patterns of the domains mentioned above, they are tentatively separated as " homogeneous anmooric " and " heterogeneous anmooric" respectively.

4.2. Fabric analyses

A) Chernozem (Photo 6 and 7)

Neither top soil(No.1) nor sub soil(No.2) of the chernozem show any clearly recognizable plasma separation. A few plasma aggregates are present but it is difficult to distinguish them from silt grains. From these micromorphological features, s-matrixes of Chernozem are considered to belong to silasepic plasmic fabric. In the top soil, intrapedal voids consist mainly of irregular orthovughs, and most of them are connected with interpedal voids. On the other hand, intrapedal voids of sub soil consist of vughs and channels(single and dendroid) and many channels have good connection with the surface of peds. Some of the channels are loosely filled up with aggregates of the same composition as the s-matrix to form aggotubules(orthotubules). In the top soil, very few sesquioxidic nodules(approximately 0.1 mm in diameter) are recognized. About this disscussion will be made later. No glaeboles were recognized in the matrix of the sub soil. Cutans are not recognized both in top soil and in sub soil.

The plasmic fabric of top soil is classified as vughy silasepic with few sesquioxidic nodules, and that of sub soil as channelled and vughy silasepic with aggotubules .

B) Dark meadow soil (Photo 8)

S-matrix of Dark meadow soil (No.3) shows the similar characteristics to those of Chernozem and is considered to belong to silasepic plasmic fabric.

Intrapedal voids consist of many dendroid channels and few vesicles.

Most of the channels are well connected with interpedal voids.

The channels sometimes include some skeleton grains or aggregates and show the tendency of transition to pedotubules. Cutans and glaeboles are not recognized. This plasmic fabric is classified as Channelled

4. Description of micromorphological features

4.1 Humusforms

A) Chernozem (Photo 1 and 2)

The thin sections of sample No.1(Chernozem, top soil) and No.2 (Chernozem, sub soil) show brown, very finely divided humus substances which are completely mixed with clay to form clay-humus complex. This clay-humus complex is homogeneously distributed in the matrix and fills up the interspace among the skeleton grains compactly. Under high magnification(X 200), it is recognizable that most of the clay-humus complexes consist of coagulated dark brown particles. Some remnants of plant tissue are present, but they are highly decomposed (brownish colour and no recognizable cell structures). Several lenticular plant residues, inside of which faint remnants of cell structure are recognizable, are present in the top soil. They are possibly the remnants of plant seed. In the subsoil, this seed remnants were not found. From the above microscopic observations, the humusform of the chernozem samples were identified as mull.

B) Dark meadow soil (Photo 3)

The thin section of sample No.3 (Dark meadow soil) shows many dark brown domains (approximately 50 μ in diameter) predominantly consisting of poorly humified plant remnants. These domains are interspersed among the finely divided clay-humus complex which is homogeneously distributed. Besides clay-humus complex, slightly decomposed plant tissues, brown in colour but with still recognizable cell structures, are present in small amount outside the peds or inside intrapedal pores.

silasepic.

C7 Black soils of Humic Gley origin(Photo 9 and 10)

Although the s-matrix of sandy Black soil of Humic Gley origin(No.4) shows some plasma separation distributed as small patches, most plasma separation occurs as channel cutans. Therefore this plasmic fabric is considered as in-vosepic.

Intrapedal voids consist mainly of dendroid channels and some vughs. A few undifferentiated sesquioxidic nodules are present near the voids. From these observations this fabric is classified as channelled in-vosepic with undifferentiated sesquioxidic nodules.

On the other hand, the s-matrix of clayey Black soil of Humic Gley origin (No.5) shows a predominant characteristic of insepic plasmic fabric. A faint and somewhat subcutanic plasma separation occurs along the margin of some channels or vesicles. This faint cutan is only recognizable at high magnification (X 200).

This plasmic fabric may be considered as vo-insepic.

Intrapedal voids are dendroid channels and vesicles. These voids are seldom connected with the interpedal voids and margin of ped is smooth. A few undifferentiated sesquioxidic and manganese nodules are present. This plasmic fabric is classified as channelled and vesicular vo-insepic with undifferentiated sesquioxidic nodules.

The micro-morphological characteristics of these five soil samples were summerized in Table 2.

Table 2. Micro-morphological characteristics of the samples.

Sample Micro- morpho- logical fea- tures	No.1 Chernozem (5 - 15cm)	No.2 Chernozem (35 - 45cm)	No.3 Dark meadow soil (0 - 40cm)	No.4 Black soil of Humic Gley origin (20 - 40cm).	No.5 Black soil of Humic Gley origin (20 - 40cm)
Fabric class	silasepic	silasepic	silasepic	in-vosepic	vo-insepic
Void type	irregular ortho vughs	vugh and channel	dendroid channel, transition to pedotubule, few vesicles	dendroid chan- nels and some vughs.	dendroid channels and vesicles
Cutans	_____	_____	_____	channel cutan	subcutanic
Pedotubules	_____	ortho agrotubule	_____	_____	_____
Glaebules	very few sesquioxidic nodules	_____	_____	a few undiffere- ntiated sesqui- oxidic nodules.	Few undiffere- ntiated sesqui- oxidic and mangan- ese nodules.
Crystallaria	_____	_____	_____	_____	_____
Subcutanic features	_____	_____	_____	_____	void cutan is some- what subcutanic.
Humusforms	mull	mull	mull - anmoor	anmooric (homogeneous)	anmooric (heterogeneous)

5. Discussion

Table 2 shows a successive change of micromorphological features in accordance with the difference of soil type.

The micromorphological features of Chernozem are represented by a mull humusform and well developed open intrapedal pore system which accords with intensive biological activity in the soil. It may be of interest to notice that sesquioxidic nodules exist, though very few in number, in the top soil of the chernozem soil. This fact probably suggests that the soil forming process occurring in the chernozem soil is developing in the direction of degraded chernozem.

The micromorphological features of Black soils of Humic Gley origin are represented by an anmooric type of humus form, cutan formation by separation, the presence of sesquioxidic nodules and the closed nature of intrapedal pore system. Especially in the case of heavy soils, the heterogeneous distribution pattern of anmooric humus substance in the s-matrix may have close relation with the heterogeneous intrapedal physico-chemical environmental conditions, such as redoxpotential. This may probably be caused by the closed intrapedal pore system.

The micromorphological features of Dark meadow soil show the intermediate characteristics between Chernozem and Black soil of Humic Gley origin.

Acknowledgment

The writer is very much grateful to Dr. F.W.G.Pijls, the director of the Netherlands Soil Survey Institute, who granted him to study micropedology at the institute. The writer is also grateful to Dr.A. Jongerius and his staff members, who kindly guided him to make this study.

REFERENCES

1. Brewer, R. (1964), Fabric and Mineral Analysis of Soils, John Wiley & Sons, Inc. New York.
2. Carl Zeiss, Nomogram to determine errors for Integration Eye Piece I, catalogue G40-195.
3. Cole, M. (1966), The Metals Research Quantimet(Q.T.M.), Microscope & Crystal Front, Vol.15, No.4, pp148-160.
4. Fisher, C., (1966), The Metals Research Image Analysing Computer, Particle size analysis conference, pp 1 - 15.
5. Jongerius, A. and Heintzberger, G., (1963), The preparation of mammoth-sized thin sections, Soil survey papers Nr.1, Neth. Soil Surv. Inst.
6. Jongerius, A. (1963), Optic-volumetric measurement on some humus forms. in Soil Organisms; edited by J.J. Doeksen and J. van der Drift, Amsterdam, pp 137-148.
7. Metals Research LTD, The Quantimet Image Analyzing Computer(Instruction manual), Cambridge, England.



Photo 1. Mull type of humusform.
Thin section in plain light. X 250
No. 1 Chernozem (5-15 cm)

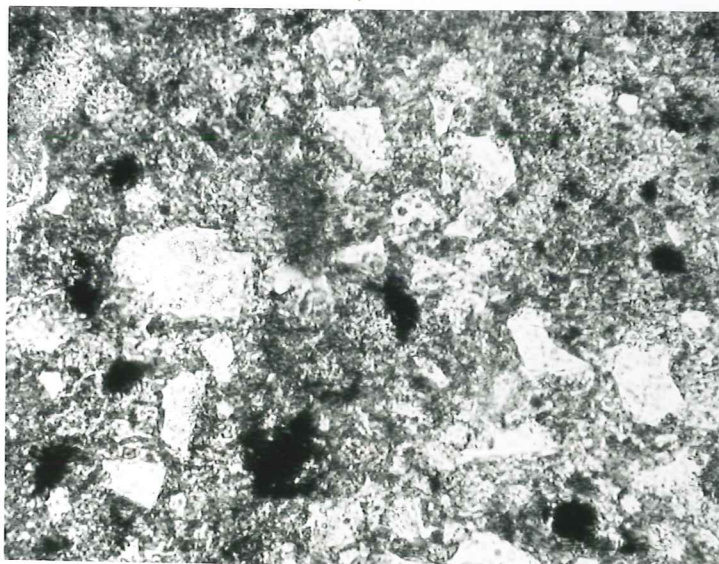


Photo 2. Mull type of humusform.
Thin section in plain light. X 250
No. 2 Chernozem (35-45 cm)

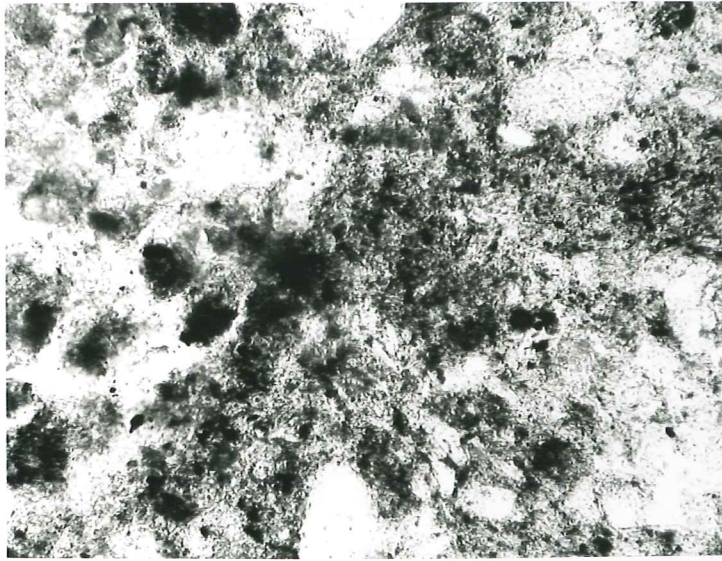


Photo 3. Transition type between mull and anmoor.
Thin section in plain light. X 250
No.3 Dark meadow soil (0-40 cm)



Photo 4. Anmooric type of humusform (homogeneous)
Thin section in plain light. X 250
No.4 Black soil of Humic Gley origin
(sandy, 20-40 cm)

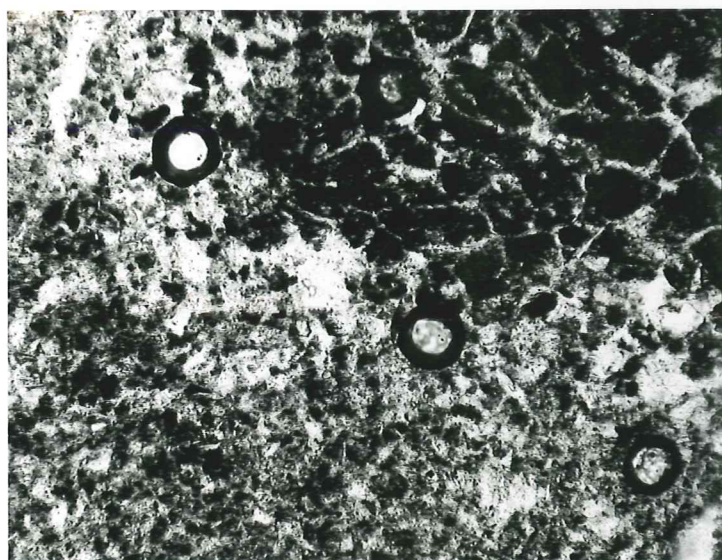


Photo 5. Anmooric type of humusform (heterogeneous)
Thin section in plain light. X 250
No.5 Black soil of Humic Gley origin
(heavy, 20-40 cm)

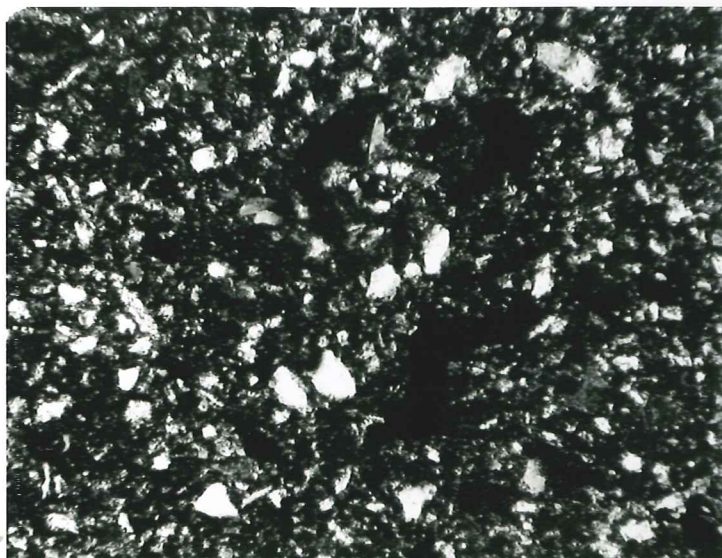


Photo 6. Vughy silasepic plasmic fabric.
Thin section under crossed polarizers. X 100
No.1 Chernozem (5-15 cm)

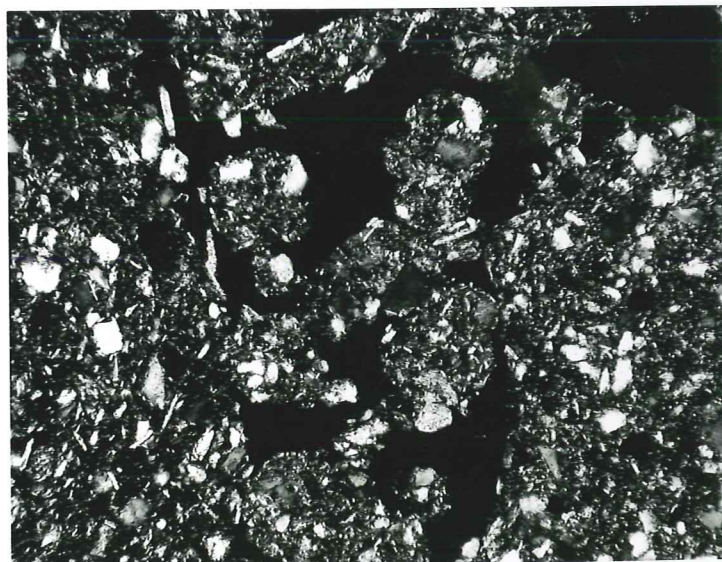


Photo 7. Silasepic plasmic fabric with aggroutubule.
Thin section under crossed polarizers. X 100
No.2 Chernozem (35-45 cm)

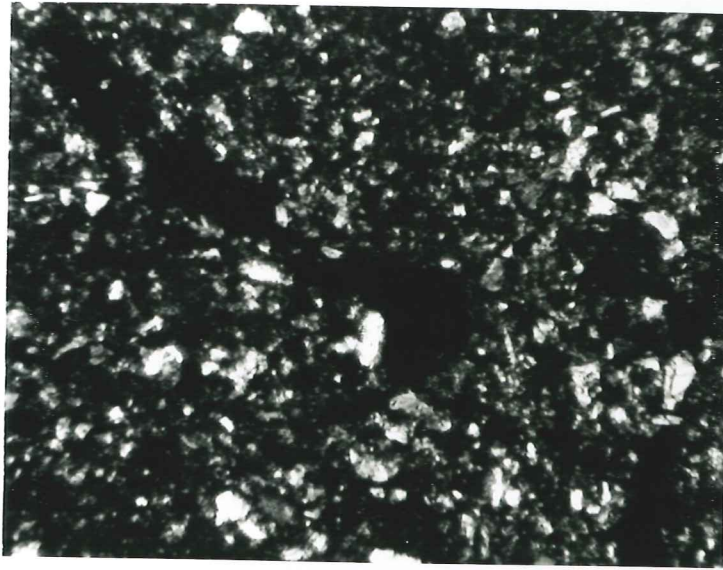


Photo 8. Channelled silasepic plasmic fabric.
Thin section under crossed polarizers. X 100
No.3 Dark meadow soil (0-40 cm)

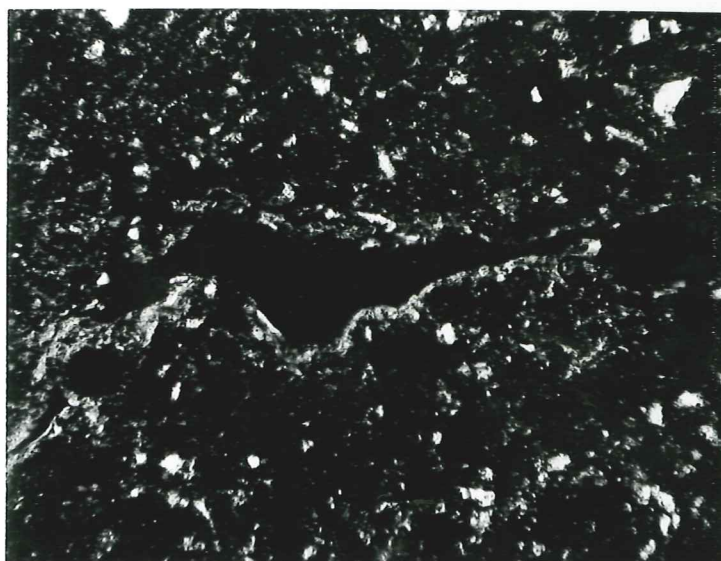


Photo 9. Channelled in-voseplic plasmic fabric.
Thin section under crossed polarizers. X 100
No.4 Black soil of Humic Gley origin.
(sandy, 20-40 cm)

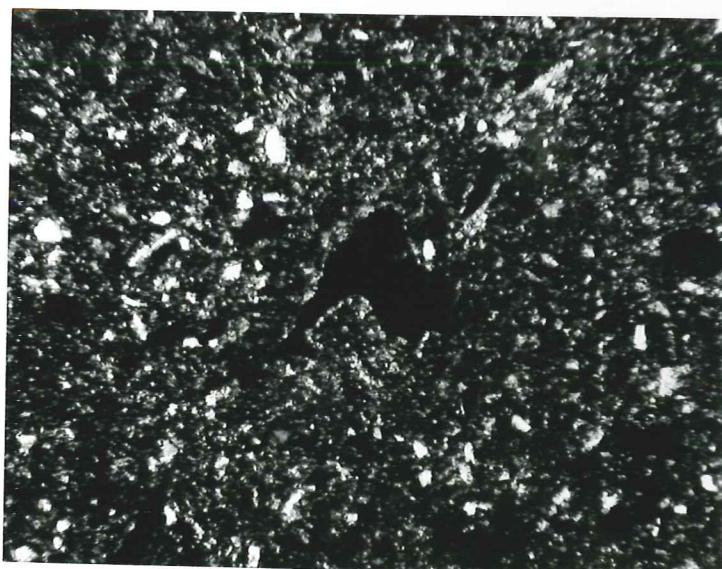


Photo 10. Vo-inseplic plasmic fabric.
Thin section under crossed polarizers. X 100
No.5 Black soil of Humic Gley origin.
(heavy, 20-40 cm)